

# Characterization of Frequency-Doubled 1.5- $\mu\text{m}$ Lasers for High-Performance Rb Clocks

Nil Almat<sup>1</sup>, William Moreno<sup>1</sup>, Matthieu Pellaton<sup>1</sup>, Florian Gruet<sup>1</sup>, Christoph Affolderbach<sup>1</sup>, *Member, IEEE*, and Gaetano Mileti<sup>2</sup>, *Member, IEEE*

**Abstract**—We report on the characterization of two fiber-coupled 1.5- $\mu\text{m}$  diode lasers, frequency-doubled and stabilized to Rubidium (Rb) atomic resonances at 780 nm. Such laser systems are of interest in view of their implementation in Rb vapor-cell atomic clocks, as an alternative to lasers emitting directly at 780 nm. The spectral properties and the instabilities of the frequency-doubled lasers are evaluated against a state-of-the-art compact Rb-stabilized laser system based on a distributed-feedback laser diode emitting at 780 nm. All three lasers are frequency stabilized using essentially identical Doppler-free spectroscopy schemes. The long-term optical power fluctuations at 780 nm are measured, simultaneously with the frequency instability measurements done by three beat notes established between the three lasers. One of the frequency-doubled laser systems shows at 780 nm excellent spectral properties. Its relative intensity noise  $<10^{-12} \text{ Hz}^{-1}$  is one order of magnitude lower than the reference 780-nm laser, and the frequency noise  $<10^6 \text{ Hz}^2/\text{Hz}$  is limited by the laser current source. Its optical frequency instability is  $<4 \times 10^{-12}$  at  $\tau = 1 \text{ s}$ , limited by the reference laser, and better than  $1 \times 10^{-11}$  at all timescales up to one day. We also evaluate the impact of the laser spectral properties and instabilities on the Rb atomic clock performance, in particular taking into account the light-shift effect. Optical power instabilities on long-term timescales, largely originating from the frequency-doubling stage, are identified as a limitation in view of high-performance Rb atomic clocks.

**Index Terms**—Clocks, diode lasers, laser stability, noise measurement, optical harmonic generation, performance evaluation, spectroscopy.

## I. INTRODUCTION

**F**REQUENCY-STABILIZED 780-nm optical sources play a crucial role in several high-precision applications in metrology [1], atomic physics and spectroscopy [2], atmospheric sensing [3], and optical telecommunication [4]. The advances in the scientific research and industrial development in these fields manifest the interest in compact, reliable, and highly stable laser sources satisfying stringent spectral requirements specific to each application. For semiconductor laser diodes (LDs) emitting at 780 nm, a widely used frequency stabilization technique consists in the use of the

rubidium (Rb) atomic absorption profile to generate the correction signal [5]. Improved laser frequency stabilities are achieved by resolving the  $^{87}\text{Rb}$  atomic transition lines close to their natural linewidths (LWs) in Doppler-free spectroscopy schemes [6], [7]. At twice the wavelength of the 780-nm Rb  $D_2$  line, corresponding to the telecommunication C-band at 1560 nm, reliable and low-cost components are available. Thus, thanks to the second-harmonic generation (SHG) technology, 1560-nm lasers can benefit from the Rb atomic reference stability at 780 nm [8]. This concept has been largely exploited in the last two decades for optical frequency references in optical telecommunication applications at 1560 nm [9], [10]. Numerous applications at 780 nm have also profited from this idea, for which the use of the frequency-doubled laser systems is demonstrated in Rb fountain clocks [11], laser cooling for atom interferometry [12], [13], ground-based gravimeter [14], onboard space applications [15], [16], and for the manipulation of the Rb with short pulses [17]. Such high-precision applications require reliable and reproducible optical sources with suitable spectral properties, which principally include the low intensity noise and frequency noise. Particularly, for Rb vapor-cell atomic clocks, the availability of such lasers emitting at 780 nm presents currently a limitation for their commercialization. In this paper, we address the application potential of the frequency-doubled laser sources to Rb vapor-cell atomic clocks.

Our group has previously developed compact and robust optical sources based on an LD emitting directly at 780 nm and Doppler-free stabilization, for applications in high-performance Rb vapor-cell clocks [18]. These optical frequency sources exhibit a frequency instability below  $10^{-11}$  up to one day of integration time. Our group also demonstrated a compact laser system based on a frequency-doubled 1560-nm LD stabilized to Rb cell reference for space-borne  $\text{CO}_2$  detection at 1572 nm [19], [20]. We also analyzed in [20] and [21] the spectral characteristics and the reproducibility of the Rb-stabilized frequency-doubled system. Thereafter, commercial lasers in the telecom C-band present convenient candidates for Rb clock applications due to the availability of reliable and reproducible high-performance components. In this paper, our principal interest concerns evaluating Rb-stabilized 1560-nm LDs combined with frequency doubling, with an emphasis on their implementation in high-performance Rb vapor-cell atomic clocks, as an alternative to optical sources emitting directly at 780 nm.

Manuscript received October 10, 2017; accepted January 9, 2018. Date of publication January 15, 2018; date of current version June 1, 2018. This work was supported in part by the Swiss National Science Foundation under Grant 156621 and Grant 162346, in part by the European Space Agency under Contract 4000106330/12/NL/EM, and in part by the Swiss Space Office, Swiss Confederation. (*Corresponding author: Nil Almat.*)

The authors are with the Laboratoire Temps-Fréquence, Institut de Physique, Université de Neuchâtel, 2000 Neuchâtel, Switzerland (e-mail: nil.almat@unine.ch; gaetano.mileti@unine.ch).

Digital Object Identifier 10.1109/TUFFC.2018.2793419

In the following, we report on the detailed characterization of two Rb-stabilized frequency-doubled laser systems based on different laser chip technologies [22]. We used as reference a light source at 780 nm. This light source is an in-house-built laser head (LH) [18], well characterized and established for high-performance Rb vapor-cell clocks. The obtained results lead to a comprehensive set of information on the frequency-doubled lasers in view of their use in many applications as cited above, with a particular emphasis on Rb vapor-cell clocks. First, we describe our experimental setup allowing the simultaneous characterization of the two frequency-doubled lasers with a single reference laser. Then, we report on the laser spectral properties followed by an analysis of the laser instabilities up to one day timescales. Finally, the impact of the three lasers' frequency and intensity fluctuations on our Rb vapor-cell atomic clock are estimated.

## II. LASER REQUIREMENTS FOR HIGH-PERFORMANCE Rb ATOMIC CLOCKS

In double-resonance (DR) Rb vapor-cell atomic clocks, the laser radiation has two purposes; optical pumping and optical detection of the Rb atomic population in the hyperfine ground states. The microwave radiation generated from a quartz oscillator is then used to interrogate the  $^{87}\text{Rb}$  clock transition  $5S_{1/2}|F=1, m_F=0\rangle \leftrightarrow 5S_{1/2}|F=2, m_F=0\rangle$  at the hyperfine splitting frequency of  $\sim 6.8347$  GHz. The frequency of the quartz oscillator is subsequently stabilized using the optically detected clock transition signal, thus improving on its frequency stability and accuracy. Passive Rb vapor-cell atomic clocks can be operated in two different schemes; in continuous-wave DR (CW-DR) [23] or pulsed optically pumped DR (POP-DR) [24]–[26]. The main difference between these two schemes is that in CW-DR the light and microwave radiations are applied to the atoms simultaneously. Whereas, in the POP-DR scheme the light is switched OFF in-between the optical pumping and detection phases, and during the microwave radiation interaction the Rb atoms are in the dark.

To satisfy the requirements for high-performance Rb vapor-cell clocks, lasers must deliver single-mode radiation at the wavelength of the  $^{87}\text{Rb}$  D<sub>1</sub> or D<sub>2</sub> line, with a mode-hop free tuning range covering several GHz. For the POP-DR scheme, the typical power required during the optical pumping phase is in a range of 15–20 mW, and during the optical detection phase of few hundreds of microwatts. In the CW-DR scheme it is on the order of few hundreds of microwatts.

The laser's spectral properties impact the clock performance at all timescales through different processes that we discuss here below [1]. On short timescales ( $\tau < 10$  s), in absence of Dick effect due to the microwave interrogation, the clock performance is mainly limited by the optical detection noise [23] which involves the shot noise, the laser amplitude modulation (AM) noise as well as the noise due to the frequency modulation (FM) noise conversion to AM noise (FM-to-AM) in the Rb vapor cell [27], [28]. In the POP scheme, additional AM noise introduced by an acousto-optic modulator, used for the light switching, may also have to be taken

into account. In order to reach a typical short-term clock frequency instability of  $2 \times 10^{-13} \tau^{-1/2}$  [23], [26] in terms of Allan deviation [29], the laser must have low relative intensity noise (RIN) level around  $10^{-11} \text{ Hz}^{-1}$  for Fourier frequencies corresponding to the clock lock-in modulation frequency, typically between 100 Hz and 1 kHz, and the FM noise below  $10^{10} \text{ Hz}^2/\text{Hz}$  for  $f = 100$  Hz.

Due to the atom interaction with light, the atomic energy levels can be shifted through the ac Stark shift [30]. This process is also known as the light shift (LS). Through the LS, the laser intensity and frequency fluctuations are transferred to the clock frequency, which represents a serious source of clock instability at all timescales. Since in the POP scheme the light and the microwave interactions are separated in time, the LS effect is considerably reduced compared to the continuous-wave operation, but still can be nonnegligible. Two distinct LS effects are observed: frequency light shift and intensity light shift. For a given clock scheme and at fixed nominal physical parameters (laser frequency and intensity, microwave power, cell temperature, etc.) the sensitivity of the clock frequency  $\nu_{\text{clock}}$  to laser frequency and intensity fluctuations can be quantified by their respective LS coefficients. The intensity LS coefficient  $\alpha$  is defined for fixed laser frequency  $\nu_L$  as expressed in (1) and the frequency LS coefficient  $\beta$  is defined for fixed laser intensity  $I_L$  as in the following equations:

$$\alpha = \Delta\nu_{\text{clock}}/\Delta I_L \quad \text{for a fixed } \nu_L \quad (1)$$

$$\beta = \Delta\nu_{\text{clock}}/\Delta\nu_L \quad \text{for a fixed } I_L. \quad (2)$$

The LS coefficients strongly depend on the clock scheme and its operational parameters. In our previous works, we presented the LS coefficient that we measured for our laser-pumped POP Rb clock in [26] and [31], and recently reported our preliminary results of the LS evaluation for each phase of the POP scheme in [22]. Taking into account the LS coefficients determined for the typical operation point of our clock [31], in order to reach instabilities at the level of  $10^{-14}$  at one day of integration time, the relative laser frequency and intensity fluctuations should not exceed  $10^{-11}$  and  $10^{-3}$ , respectively.

Our motivation for this paper lies on these aspects. The spectral characteristics (see Section IV) and the long-term fluctuations (see Section V) of the two frequency-doubled lasers are evaluated in detail considering their application in Rb vapor-cell clocks.

## III. EXPERIMENTAL SETUP

The scheme of the experimental system used to study two commercial fiber-pigtailed LDs in the telecom C-band is shown in Fig. 1. The two lasers are designed with different technologies to emit at 1560 nm: Laser-1 (RIO Planex) consists of an external cavity LD and Laser-2 (Emcore) of a distributed-feedback (DFB) LD. The first laser offers a kilohertz-level LW for a relatively higher cost while the second laser is a lower cost solution with LW on the megahertz level. Both lasers seed two nominally identical fibered optical paths. For frequency doubling through SHG, 34-mm long periodically poled lithium niobate waveguides are used. The optical

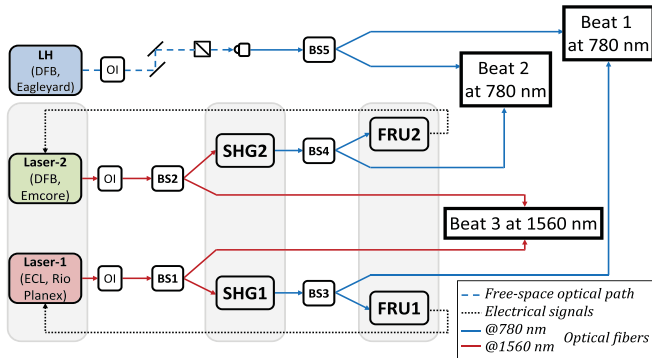


Fig. 1. Scheme of the experimental setup using two frequency-doubled lasers, Laser-1 in red and Laser-2 in green with the reference LH in blue. The same color code is applied to all graphs presenting results obtained for the three laser systems. OI: optical isolator, BS: fibered coupler here used as beam splitter, SHG: second-harmonic generation unit, FRU: frequency reference unit.

power of the second-harmonic output  $P_{\text{out}}$  has a quadratic relation with the input power  $P_{\text{in}}$  of the crystal characterized by the conversion efficiency  $\eta$  as follows:

$$P_{\text{out}} = \eta P_{\text{in}}^2. \quad (3)$$

The conversion efficiency, strongly depending on the nonlinear crystal properties, is 287%/W for SHG1 (used with Laser-1) and 319%/W for SHG2 (with Laser-2). The frequency-doubled laser frequencies are stabilized to Rb reference cells situated in the home-built frequency reference units (FRUs) using lock-in detection with laser current modulation at 50 kHz and a proportional-integrator servo loop. Each FRU includes an evacuated Rb reference cell (19-mm length and 10-mm diameter), aligned in a Doppler-free absorption scheme with compact optics, and two photodetectors (one for Doppler-free detection and the other for monitoring the dc light level at the entrance of the cell). The reference cell as well as the base plate holding the components are temperature controlled. Polarization-maintaining fused couplers implemented before and after the frequency-doubling act as beam splitter (BS) and allow accessing the light at both wavelengths of 780 and 1560 nm. The BSs have a ratio of 50/50, except BS3 that has a ratio of 90/10 to guarantee the required optical pump power for Laser-1 frequency stabilization. Main advantages of the fibered paths, compared to free-space systems, include the compactness, modularity, easier optical alignment and a reduced sensitivity of the optical alignment to vibrations.

The third laser used as the reference laser consists of our well-characterized LH [18]. It is based on a free-space DFB LD (Eagleyard Photonics) emitting at 780 nm that is frequency stabilized to a third dedicated evacuated Rb reference cell, in a similar scheme as in FRUs. The BS5 (see Fig. 1), splitting the fiber-coupled LH output in two equal parts, allows the simultaneous characterization of both frequency-doubled lasers using one single reference LH. Thanks to the simultaneously available three beat notes, called in this paper as Beat-1 and Beat-2 at 780 nm and Beat-3 at 1560 nm, the LW or frequency instability measurements can be carried out simultaneously for the three lasers.

TABLE I  
SMSR MEASURED FOR THE THREE LASER SYSTEMS AT TWO WAVELENGTHS

|                        | 1560 nm | 780 nm  |
|------------------------|---------|---------|
| <i>Laser-1</i>         | 54 dB   | > 62 dB |
| <i>Laser-2</i> [21]    | 44 dB   | > 60 dB |
| <i>Laser head</i> [18] | -       | > 40 dB |

#### IV. LASER SPECTRAL CHARACTERIZATION

The lasers' spectral properties are analyzed with an emphasis on applications to Rb vapor-cell clocks. First, the general parameters of the laser systems' outputs are discussed, then, the RIN and FM noise measurements. Finally, the laser LWs are evaluated using two different methods.

##### A. Basic Parameters

Laser-1 output power detected at 1560 nm is around 15 mW, and 27 mW for Laser-2, at injection currents of 168 and 183 mA, and laser temperatures of 24.0 °C and 25.8 °C, respectively. In the configuration depicted in Fig. 1, the optical powers of the light at 780 nm used for the beat notes with the frequency-doubled lasers are 18 and 900  $\mu\text{W}$ , respectively, for Laser-1 and Laser-2.

Table I presents the side-mode suppression ratios (SMSRs) measured for all three laser systems using an optical spectrum analyzer. The SMSR for the laser outputs at 1560 nm is comparable with the one measured for the 780-nm LH. After the frequency doubling, the SMSR is significantly improved by more than 20 dB, thanks to the narrow efficiency curves ( $\sim 50$  GHz) of the SHG in the nonlinear crystal.

##### B. RIN

We measure the laser intensity noise power spectral density (PSD) up to 100-kHz Fourier frequencies with a fast Fourier transform spectrum analyzer. The RIN determined for the three lasers at both wavelengths are compared in Fig. 2 along with the required noise level allowing a clock short-term frequency instability of  $2 \times 10^{-13} \tau^{-1/2}$ . Close to 100-kHz Fourier frequencies, the measured PSD for the frequency-doubled lasers is limited by the photodetector bandwidth and the one measured for LH by the photodetector intrinsic noise. All three laser systems satisfy the RIN requirements for most of the applications mentioned in the first section. Due to the quadratic dependence of the second-harmonic power at 780 nm on the 1560-nm SHG input power as in (3), the RIN is increased by a factor of  $2^2$  with respect to the one measured at 1560 nm for the frequency-doubled lasers. These results show that no significant other additional noise is introduced during the SHG process. The RIN for the frequency-doubled Laser-2 is measured similar to LH. For Laser-1, RIN at 780 nm is one order of magnitude lower at all Fourier frequencies.

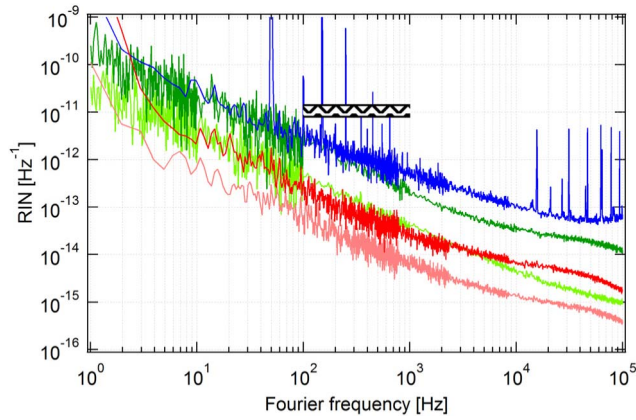


Fig. 2. RIN measured at 780 and 1560 nm for the three laser systems. Light red: Laser-1 and light green: Laser-2 at 1560 nm, red: Laser-1 and green: Laser-2 at 780 nm, and blue: 780-nm LH where the spikes originate from the photo-detector circuit. Black wavy area: specification for the RIN to reach the short-term clock instability of  $2 \times 10^{-13} \tau^{-1/2}$  for a clock lock-in modulation frequency between 100 Hz and 1 kHz.

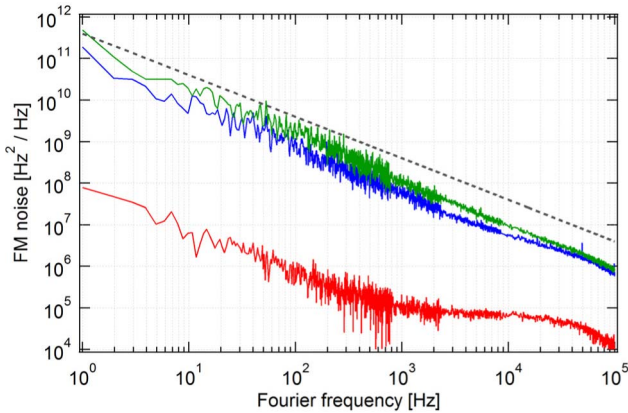


Fig. 3. FM noise of the free-running lasers measured at 780 nm. Red: Laser-1, green: Laser-2, and blue: LH. Black dashed line: specification required for Rb vapor-cell atomic clocks.

### C. FM Noise

The FM noise at 780 nm is determined via the PSD of a laser tuned to the slope of the Rb Doppler absorption profile obtained from a separate Rb cell. The slope of the absorption line acts as a frequency discriminator and converts the FM noise into AM noise. Fig. 3 shows the FM noise spectra measured at 780 nm for the three free-running lasers with the same optical powers ( $31.5 \pm 1.5 \mu\text{W}$ ) entering the separate Rb cell. The FM noise for Laser-2 is at similar order of magnitude than the one for LH. For Laser-1, the FM noise at 780 nm is at least two orders of magnitude lower, which is currently limited by the noise of the laser current source ( $1 \text{ nA}/\text{Hz}^{1/2}$ ). We also measured the FM noise for the frequency-stabilized lasers at 780 nm. In this case, for the three lasers the FM noise is reduced below  $10^8 \text{ Hz}^2/\text{Hz}$  for Fourier frequencies up to the lock bandwidth of each system which is between 2 and 5 kHz.

### D. Linewidth

The laser LWs at 780 nm gathered in Table II are determined by two different methods. The first method consists of measuring the LW of the three heterodyne beat-note signals

TABLE II  
LASER LWs MEASURED AT 780 nm

|            | From beat-note signal<br>[MHz] | Beta-line method<br>[MHz] |
|------------|--------------------------------|---------------------------|
| Laser-1    | $0.6 + 1.1 / - 0.6$            | $0.15 \pm 0.02$           |
| Laser-2    | $2.0 \pm 1.1$                  | $3.20 \pm 0.32$           |
| Laser head | $2.1 \pm 1.1$                  | $2.24 \pm 0.22$           |

using an RF spectrum analyzer. The individual laser LWs are deduced from the three-equation system and the error bars determined by standard uncertainty propagation. The second one exploits the beta-separation line method [32] based on the measured FM noise spectra discussed in Section IV-C. The LWs calculated with the second method are in good agreement with [18] and [20], respectively, for LH and Laser-2. For Laser-1, the measurement is limited by the current source noise and corresponds to the equivalent in FM noise of the laser current source noise (FM noise level expected from the current noise multiplied by the laser's frequency-current tuning coefficient). The LW at 780 nm is expected to be on the order of few kilohertz based on the datasheet indications (1.4 kHz at 1560 nm). Assuming no additional noise, the LW of the frequency-doubled output is increased by a factor of two due to the quadratic dependence of the SHG described in (3). With the first-mentioned method, the LW measurements for Laser-1 are dominated by the larger LWs of Laser-2 and LH. To avoid the modulation effects on the measured LWs, the laser current modulation is switched OFF, thus the lasers are in free-running mode (open-loop conditions). The laser frequency fluctuations in this mode lead to the relatively large error bars (see Table II) which present a limitation for this method when considering narrow LWs. Yet, the results are reasonably consistent between the two methods.

## V. LASER FREQUENCY AND POWER INSTABILITIES

Long-term measurements of the laser frequency and optical power fluctuations were carried out in the configuration of three simultaneous beat notes shown in Fig. 1. The stabilization loop parameters, which have a direct impact on the signal-to-noise ( $S/N$ ) limit of the laser frequency instability, were optimized for each laser system separately. The beat-note frequency repeatability, for different Doppler-free feature locking points chosen for the lasers, is between 10 and 100 kHz, which is in good agreement with [21].

### A. Frequency Instability

The relative frequency fluctuations measured for three beat notes are shown in terms of the overlapping Allan deviation in Fig. 4 along with the specification needed for a high-performance Rb clock. At 1 s of integration time, the frequency instabilities, measured below  $5 \times 10^{-12}$  for both beat notes against the LH, appear to be limited by the reference LH itself. The  $S/N$  limits for each of the three laser systems

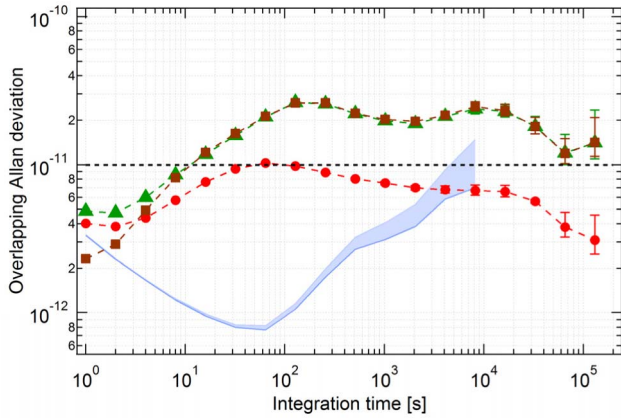


Fig. 4. Relative frequency fluctuations in terms of overlapping Allan deviation for the three simultaneous beat-note frequency measurements. Red dots: Beat-1 at 780 nm, green triangles: Beat-2 at 780 nm, brown squares: Beat-3 at 1560 nm, and blue area: heterodyne beat-note between two identical LHs, as reference. Black dashed line: specification required for high-performance Rb vapor-cell atomic clocks.

are estimated from the respective lock-in correction signal and the detection noise at the modulation frequency for each laser system [27]. For the two beat notes at 780 nm, Beat-1 and Beat-2, the measured instabilities at 1 s agree well with the estimated LH  $S/N$  limit of  $3.7 \times 10^{-12} \tau^{-1/2}$  and, for the Beat-3, with the estimated Laser-2  $S/N$  limit of  $1.5 \times 10^{-12} \tau^{-1/2}$ . For Laser-1, the  $S/N$  limit prediction is one order of magnitude lower, at  $2.5 \times 10^{-13} \tau^{-1/2}$ .

For integration times  $\tau > 10$  s, fully overlapping Beat-2 and Beat-3 Allan variances (see Fig. 4) confirm the high relative frequency fluctuations of the Laser-2 system. Thanks to the modularity of our experimental system, we could investigate the instability contribution at each stage of the two fibered paths and our efforts are ongoing considering the Laser-2 system but, so far we can exclude the contributions from the SHG unit and the FRU.

In the mid-term ( $10 < \tau < 100$  s), the Laser-1 instability is limited by the optical reflections in the fibered system leading to etalon fringes superimposed on the absorption profile used for the lock in. In principle, it should be possible to suppress the etalon fringes by an appropriate signal subtraction circuit to improve on the mid-term Laser-1 frequency stability. Finally, in the long-term ( $\tau = 10^4$  s), the main limitation comes from the thermal fluctuations in the laboratory.

### B. Optical Power Instability

For all three laser systems, the optical power at 780 nm (before the Rb reference cells) is measured simultaneously to the beat-note frequency measurements discussed in Section V-A. The relative fluctuations in terms of the overlapping Allan deviation are plotted in Fig. 5. On long-term timescales ( $\tau > 10^4$  s), the two frequency-doubled laser systems show power fluctuations of more than 0.1% at  $\tau = 10^4$  s, while the free-space LH shows close to two orders of magnitude lower optical power instability ( $< 0.02\%$  for  $\tau$  up to  $10^5$  s). This optical power instability of the frequency-doubled laser systems at long-term timescales currently puts a

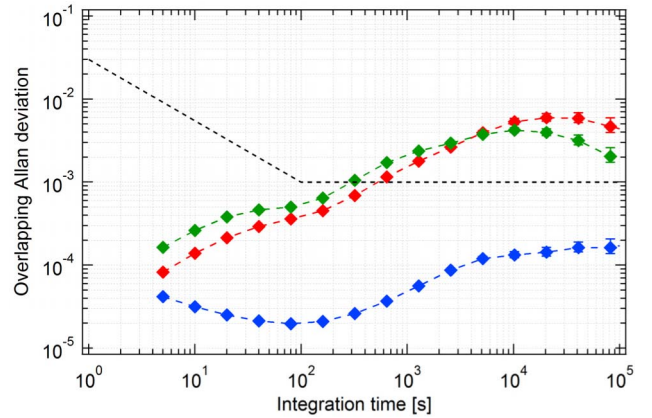


Fig. 5. Relative optical power fluctuations, measured simultaneously before the Rb reference cells, plotted in terms of overlapping Allan deviation. Red: Laser-1, green: Laser-2, and blue: LH. Black dashed line: specification required for Rb vapor-cell atomic clocks.

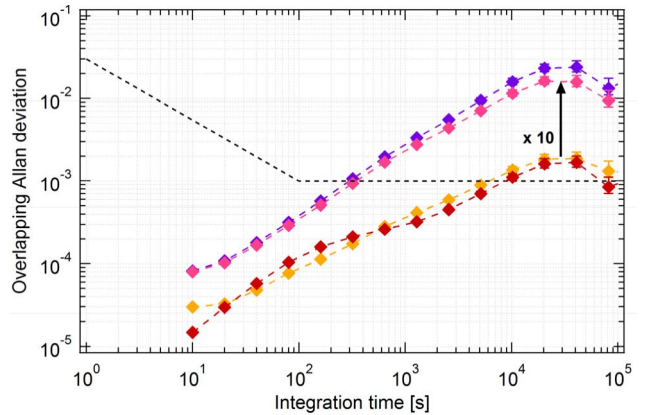


Fig. 6. Relative optical power fluctuations, detected at each stage of the Laser-1 system, in terms of overlapping Allan deviation. Dark red: LD output at 1560 nm, yellow: BS1 output at 1560 nm, purple: BS3 output at 780 nm, and magenta: before the Rb reference cell at 780 nm. Black dashed line: specification required for Rb vapor-cell atomic clocks.

limitation to their use in Rb high-performance atomic clocks, but an active optical power stabilization could reduce these fluctuations.

To identify the origin of this power instability level, we measured the optical power fluctuations at each stage of the Laser-1 frequency stabilization chain. The relative fluctuations of the optical power in terms of the overlapping Allan deviation are shown in Fig. 6. According to our results, the fibered couplers do not induce significant additional fluctuations. However, during the frequency-doubling stage, the optical power instability is degraded by a factor of 10, in contrast to a degradation by a factor of 2 expected from the SHG process [first-order derivative of (3)]. We also observed that the optical power fluctuations are correlated with the variations of the laboratory temperature, which indicates that thermal effects are likely at the origin of the measured power instabilities.

## VI. APPLICATION TO Rb VAPOR-CELL ATOMIC CLOCKS

In this section, we estimate the impact of the laser spectral properties and its frequency and intensity long-term fluctuations on the performance of our POP Rb atomic clock.

TABLE III  
ESTIMATED LASER FREQUENCY AND INTENSITY FLUCTUATIONS IMPACT TO THE CLOCK INSTABILITY

| (for $\tau = 10^4$ s) | Frequency LS           |   | Intensity LS                    |   | Estimated total clock instability due to light-shifts |
|-----------------------|------------------------|---|---------------------------------|---|---|
|                       | Frequency fluctuations | Estimated contribution to clock instability | Relative intensity fluctuations | Estimated contribution to clock instability |   |
| Laser-1               | 3 kHz                  | $1.4 \times 10^{-15}$                       | 0.5 %                           | $1.1 \times 10^{-14}$                       | $1.1 \times 10^{-14}$                                 |
| Laser-2               | 10 kHz                 | $4.6 \times 10^{-15}$                       | 0.6 %                           | $1.3 \times 10^{-14}$                       | $1.3 \times 10^{-14}$                                 |
| Laser head            | 4 kHz                  | $1.8 \times 10^{-15}$                       | 0.02 %                          | $4.2 \times 10^{-16}$                       | $4.2 \times 10^{-16}$                                 |

### A. Impact on the Short-Term Clock Instability

On short timescales ( $\tau < 10$  s), the ultimately dominant clock instability source is the optical detection noise that is typically dominated by the FM-to-AM noise conversion through the Rb clock cell [26]. The noise conversion factor depends strongly on the Rb clock cell temperature as well as the precise laser frequency [27], [28]. Here, we estimate the change of the clock detection noise when using different laser sources, while maintaining constant the FM-to-AM conversion, i.e., the clock cell temperature and the laser frequency.

The RIN and FM noises for Laser-2 measured at 780 nm are of the same order of magnitude as those for the LH. For typical clock operation parameters, comparable short-term clock performance may be expected in the case where Laser-2 is used for the optical pumping and detection in the clock. For Laser-1, we measured the RIN at 780-nm one order of magnitude lower than the other two lasers. Also, its FM noise, currently limited by the current source noise, is more than two orders of magnitude lower than the one of the LH up to 1-kHz Fourier frequencies. With these results and assuming a similar FM-to-AM conversion factor through the Rb clock cell, AM and FM noise contributions to the short-term clock instability are expected to be considerably reduced with Laser-1 and probably become a negligible instability source for the short-term clock performance.

### B. Impact on the Long-Term Clock Instability

The contribution of the long-term laser instabilities to the clock performance via the LS is estimated using the LS coefficients. For typical operating parameters of our POP Rb clock, the LS coefficients, as defined in Section II, are  $\alpha = -2.1 \times 10^{-14}/\%$  and  $\beta = 4.6 \times 10^{-16}/\text{kHz}$  [31]. Table III summarizes the estimated contributions to the clock instability for simultaneously measured laser frequency and power fluctuations. The impact of the laser frequency fluctuations, measured to be  $<4$  kHz (relative fluctuations below  $10^{-11}$ ), is negligible for all three laser systems in view of the long-term clock instability. The intensity LS appears to be the main limitation for the clock instability with the frequency-doubled lasers as optical source. An active power stabilization could reduce this effect.

## VII. CONCLUSION

We reported on the performance evaluation of two frequency-doubled and Rb-stabilized 1560-nm LDs based on

different technologies, in view of their application to Rb vapor-cell atomic clocks, as an alternative to 780-nm lasers. The RIN and FM noise of the frequency-doubled Laser-1, determined at 780 nm, are more than one order of magnitude lower than the reference laser based on an LD emitting directly at 780 nm. This observation makes Laser-1 a highly interesting candidate for implementation in a Rb vapor-cell atomic clock. Furthermore, the low frequency instability, better than  $10^{-11}$  at all timescales, of Laser-1 leads to a highly stable double-wavelength optical frequency source for many applications, in particular for Rb vapor-cell clocks. However, the frequency instability for Laser-2 is limited in the mid- and long-terms. The optical power instability for both frequency-doubled lasers, transferred to the clock instability via the intensity LS, currently presents a limitation for their use in Rb vapor-cell atomic clocks. Moreover, the Grosslambert crossvariance analysis [33], [34] could allow identifying the individual laser system instabilities, in our case with one low-noise laser compared to two similar higher noise ones, and can be considered in our future studies.

The measured spectral properties and frequency instability for the frequency-doubled Laser-1 system are very promising in view of high-performance Rb vapor-cell clocks, though, an active optical power stabilization scheme must be considered to reduce the impact of the long-term optical power fluctuations on the Rb atomic clock stability. Furthermore, amplification of the 780-nm laser radiation to the power levels required for Rb atomic clocks needs to be considered, as well as the implementation of optical switching means for the laser radiation applied to the atoms for the POP scheme.

## ACKNOWLEDGMENT

The authors would like to thank Dr. R. Matthey for his previous work and M. Durrenberger and P. Scherler for their technical support. They would also like to thank the reviewers for their helpful suggestions.

## REFERENCES

- [1] J. Vanier and C. Mandache, "The passive optically pumped Rb frequency standard: The laser approach," *Appl. Phys. B*, vol. 87, no. 4, pp. 565–593, 2007.
- [2] C. E. Wieman and L. Hollberg, "Using diode lasers for atomic physics," *Rev. Sci. Instrum.*, vol. 62, no. 1, pp. 1–20, 1991.
- [3] K. Numata, J. R. Chen, S. T. Wu, J. B. Abshire, and M. A. Krainak, "Frequency stabilization of distributed-feedback laser diodes at 1572 nm for lidar measurements of atmospheric carbon dioxide," *Appl. Opt.*, vol. 50, no. 7, pp. 1047–1056, Mar. 2011.

- [4] M. Nakazawa, "Recent progress on ultrafast/ultrashort/frequency-stabilized erbium-doped fiber lasers and their applications," *Frontiers Optoelectron. China*, vol. 3, no. 1, pp. 38–44, Mar. 2010.
- [5] M. Têtu, B. Villeneuve, N. Cyr, P. Tremblay, S. Thériault, and M. Breton, "Multiwavelength sources using laser diodes frequency-locked to atomic resonances," *J. Lightw. Technol.*, vol. 7, no. 10, pp. 1540–1548, Oct. 1989.
- [6] O. Schmidt, K.-M. Knaak, R. Wynands, and D. Meschede, "Cesium saturation spectroscopy revisited: How to reverse peaks and observe narrow resonances," *Appl. Phys. B*, vol. 59, no. 2, pp. 167–178, Aug. 1994.
- [7] C. Affolderbach, C. Andreeva, S. S. Cartaleva, G. Mileti, and D. G. Slavov, "Frequency stability comparison of diode lasers locked to Doppler and sub-Doppler resonances," *Proc. SPIE*, vol. 5449, pp. 1–8, Jun. 2004.
- [8] M. Ohtsu and E. Ikegami, "Frequency stabilisation of 1.5  $\mu\text{m}$  DFB laser using internal second harmonic generation and atomic  $^{87}\text{Rb}$  line," *Electron. Lett.*, vol. 25, no. 1, pp. 22–23, Jan. 1989.
- [9] M. Poulin, N. Cyr, C. Latrasse, and M. Têtu, "Progress in the realization of a frequency standard at 192.1 THz (1560.5 nm) using  $^{87}\text{Rb}$  D2-line and second harmonic generation," *IEEE Trans. Instrum. Meas.*, vol. 46, no. 2, pp. 157–161, Apr. 1997.
- [10] Y. Han, S. Guo, J. Wang, H. Liu, J. He, and J. Wang, "Efficient frequency doubling of a telecom 1560 nm laser in a waveguide and frequency stabilization to Rb D2 line," *Chin. Opt. Lett.*, vol. 12, no. 12, p. 121401, Dec. 2014.
- [11] S. Peil, S. Crane, T. Swanson, and C. R. Ekstrom, "The USNO rubidium fountain," in *Proc. IEEE IFCS*, Jun. 2006, pp. 304–306.
- [12] R. J. Thompson, M. Tu, D. C. Aveline, N. Lundblad, and L. Maleki, "High power single frequency 780 nm laser source generated from frequency doubling of a seeded fiber amplifier in a cascade of PPLN crystals," *Opt. Exp.*, vol. 11, no. 14, pp. 1709–1713, Jul. 2003.
- [13] F. Theron, Y. Bidel, E. Dieu, N. Zahzam, M. Cadoret, and A. Bresson, "Frequency-doubled telecom fiber laser for a cold atom interferometer using optical lattices," *Opt. Commun.*, vol. 393, pp. 152–155, Jun. 2017.
- [14] Q. Wang, Z. Wang, Z. Fu, W. Liu, and Q. Lin, "A compact laser system for the cold atom gravimeter," *Opt. Commun.*, vol. 358, pp. 82–87, Jan. 2016.
- [15] O. Carraz *et al.*, "Compact and robust laser system for onboard atom interferometry," *Appl. Phys. B*, vol. 97, no. 2, p. 405, Aug. 2009.
- [16] T. Lévêque, L. Antoni-Micollier, B. Faure, and J. Berthon, "A laser setup for rubidium cooling dedicated to space applications," *Appl. Phys. B*, vol. 116, no. 4, pp. 997–1004, Sep. 2014.
- [17] J. Dingjan *et al.*, "A frequency-doubled laser system producing ns pulses for rubidium manipulation," *Appl. Phys. B*, vol. 82, no. 1, pp. 47–51, Jan. 2006.
- [18] F. Gruet, M. Pellaton, C. Affolderbach, T. Bandi, R. Matthey, and G. Mileti, "Compact and frequency stabilized laser heads for Rubidium atomic clocks," *Proc. SPIE*, vol. 10564, p. 105642Y, Nov. 2017.
- [19] R. Matthey, W. Moreno, F. Gruet, P. Brochard, S. Schilt, and G. Mileti, "Rb-stabilized laser at 1572 nm for  $\text{CO}_2$  monitoring," *J. Phys., Conf. Ser.*, vol. 723, no. 1, p. 012034, 2016.
- [20] W. Moreno, R. Matthey, F. Gruet, P. Brochard, S. Schilt, and G. Mileti, "Rb-stabilized optical frequency reference at 1572 nm," in *Proc. EFTF*, Apr. 2016, pp. 1–4.
- [21] W. Moreno, R. Matthey, F. Gruet, P. Brochard, S. Schilt, and G. Mileti, "Rb-stabilized compact optical frequency comb acting as a versatile wavelength reference," in *Proc. CLEO*, Jun. 2016, p. SM2H.5.
- [22] N. Almat *et al.*, "Cell-based stabilized laser sources and light-shifts in pulsed Rb atomic clocks," in *Proc. IFCS-EFTF*, Jul. 2017, pp. 63–65.
- [23] T. Bandi, C. Affolderbach, C. Stefanucci, F. Merli, A. K. Skrivervik, and G. Mileti, "Compact high-performance continuous-wave double-resonance rubidium standard with  $1.4 \times 10^{-13} \text{ T}^{-1/2}$  stability," *IEEE Trans. Ultrason., Ferroelect., Freq. Control*, vol. 61, no. 11, pp. 1769–1778, Nov. 2014.
- [24] S. Micalizio, A. Godone, C. Calosso, F. Levi, C. Affolderbach, and F. Gruet, "Pulsed optically pumped rubidium clock with high frequency-stability performance," *IEEE Trans. Ultrason., Ferroelect., Freq. Control*, vol. 59, no. 3, pp. 457–462, Mar. 2012.
- [25] S. Micalizio, C. E. Calosso, A. Godone, and F. Levi, "Metrological characterization of the pulsed Rb clock with optical detection," *Metrologia*, vol. 49, no. 4, pp. 425–436, 2012.
- [26] S. Kang, M. Gharavipour, C. Affolderbach, F. Gruet, and G. Mileti, "Demonstration of a high-performance pulsed optically pumped Rb clock based on a compact magnetron-type microwave cavity," *J. Appl. Phys.*, vol. 117, no. 10, p. 104510, 2015.
- [27] G. Mileti and P. Thomann, "Study of the S/N performance of passive atomic clocks using a laser pumped vapour," in *Proc. EFTF*, 1995, pp. 271–276.
- [28] J. C. Camparo, "Conversion of laser phase noise to amplitude noise in an optically thick vapor," *J. Opt. Soc. Amer. B, Opt. Phys.*, vol. 15, no. 3, pp. 1177–1186, 1998.
- [29] D. W. Allan, "Statistics of atomic frequency standards," *Proc. IEEE*, vol. 54, no. 2, pp. 221–230, Feb. 1966.
- [30] C. Cohen-Tannoudji, "Théorie quantique du cycle de pompage optique. vérification expérimentale des nouveaux effets prévus," Ph.D. dissertation, Faculté des Sci., Univ. Paris, Paris, France, 1962.
- [31] M. Gharavipour *et al.*, "High performance vapour-cell frequency standards," *J. Phys., Conf. Ser.*, vol. 723, no. 1, p. 012006, 2016.
- [32] G. Di Domenico, S. Schilt, and P. Thomann, "Simple approach to the relation between laser frequency noise and laser line shape," *Appl. Opt.*, vol. 49, no. 25, pp. 4801–4807, Sep. 2010.
- [33] J. Gros Lambert, D. Fest, M. Olivier, and J. J. Gagnepain, "Characterization of frequency fluctuations by crosscorrelations and by using three or more oscillators," in *Proc. IEEE IFCS*, May 1981, pp. 458–463.
- [34] F. Vernotte, C. E. Calosso, and E. Rubiola, "Three-cornered hat versus Allan covariance," in *Proc. IEEE IFCS*, May 2016, pp. 1–6.



**Nil Almat** received the M.S. degree in micro-engineering from the École Polytechnique Fédérale de Lausanne, Lausanne, Switzerland, in 2014. She is currently pursuing the Ph.D. degree in physics with the Laboratoire Temps-Fréquence, University of Neuchâtel, Neuchâtel, Switzerland.

She joined Alpes Lasers SA, St. Blaise, Switzerland, as a Research and Development Engineer in 2015. Her current research interests include atomic spectroscopy, frequency-stabilized lasers, and vapor-cell atomic clocks.



**William Moreno** received the M.S. degree in physics from the École Polytechnique Fédérale de Lausanne, Lausanne, Switzerland, in 2014. He is currently pursuing the Ph.D. degree with the Laboratoire Temps-Fréquence, University of Neuchâtel, Neuchâtel, Switzerland, where he focused on atomic clock and frequency-stabilized lasers.



**Matthieu Pellaton** received the M.S. and Ph.D. degrees in physics from the University of Neuchâtel, Neuchâtel, Switzerland, in 2008 and 2014, respectively.

From 2015 to 2016, he was a Scientific Collaborator with the Optics Laboratory, Swiss Federal Institute of Metrology METAS, Berne-Wabern, Switzerland. In 2017, he joined the Laboratoire Temps-Fréquence, University of Neuchâtel, where he is currently a Post-Doctoral Researcher.

His current research interests include atomic spectroscopy, microwave resonator, and vapor-cell atomic frequency standards, particularly, miniaturized frequency standards and laser-pumped high-performance atomic clocks.



**Florian Gruet** received the Diploma degree in microtechnics engineering from the Specialized Engineer School, Le Locle, Switzerland, in 2008.

In 2008, he joined the Laboratoire Temps-Fréquence, University of Neuchâtel, Neuchâtel, Switzerland, as a Scientific Collaborator. His current research interests include optical systems and stabilized lasers.



**Christoph Affolderbach** (M'13) received the Diploma and Ph.D. degrees in physics from Bonn University, Bonn, Germany, in 1999 and 2002, respectively.

From 2001 to 2006, he was a Research Scientist at the Observatoire Cantonal de Neuchâtel, Neuchâtel, Switzerland. In 2007, he joined the Laboratoire Temps-Fréquence, University of Neuchâtel, Neuchâtel, where he is currently a Senior Scientific Collaborator. His current research interests include the development of stabilized diode laser systems,

atomic spectroscopy, and vapor-cell atomic frequency standards, particularly, laser-pumped high-performance atomic clocks and miniaturized frequency standards.



**Gaetano Mileti** (M'12) received the Diploma degree in physics from the École Polytechnique Fédérale de Lausanne, Lausanne, Switzerland, in 1990, and the Ph.D. degree in physics from the University of Neuchâtel, Neuchâtel, Switzerland, in 1995. From 1991 to 1995 and from 1997 to 2006, he was a Research Scientist at the Observatoire Cantonal de Neuchâtel, Neuchâtel. From 1995 to 1997, he was with National Institute of Standards and Technology, Boulder, CO, USA. In 2007, he co-founded the Laboratoire Temps-Fréquence, University of Neuchâtel,

Neuchâtel, Switzerland, where he is currently the Deputy Director and an Associate Professor. His current research interests include atomic spectroscopy, stabilized lasers, and frequency standards.